

# Kramers theory in the relaxation dynamics of a tilted asymmetric periodic potential

Takaaki Monnai,<sup>1,\*</sup> Ayumu Sugita,<sup>2,†</sup> and Katsuhiko Nakamura<sup>2,‡</sup>

<sup>1</sup>*Department of Applied Physics, Waseda University, 3-4-1 Okubo, Shinjuku-ku, Tokyo 169-8555, Japan*

<sup>2</sup>*Department of Applied Physics, Osaka City University, 3-3-138 Sugimoto, Sumiyoshi-ku, Osaka 558-8585, Japan*

(Received 10 April 2007; published 28 September 2007)

We investigate the low-temperature relaxation dynamics toward a nonequilibrium steady state in a tilted asymmetric periodic potential based on the WKB analysis and the numerical diagonalization of the Fokker-Planck operator. Due to the tilting, the Fokker-Planck operator, and thus the Schrödinger operator associated with it, are non-Hermitian. Therefore, we evaluate the decay rate based on the WKB analysis both for real- and complex-valued eigenvalues. In the tilting range where the double-humped barrier exists, the decay rate is shown to obey a law which is a subtle nonequilibrium extension of the so-called Kramers escape rate. The decay rate for the single-humped barrier case is analyzed as well. The large tilting regime where the barriers no longer exist is also investigated.

DOI: [10.1103/PhysRevE.76.031140](https://doi.org/10.1103/PhysRevE.76.031140)

PACS number(s): 05.40.-a, 05.70.Ln, 82.20.Db

## I. INTRODUCTION

The low-temperature dynamics in the free energy landscape [1–3] can be treated as the escape processes of a Brownian particle over the barriers [4–9] and thus as the relaxation dynamics towards the thermal equilibrium or the nonequilibrium steady state.

In the context of relaxation to the well-defined thermal equilibrium, a subtle extension of the Kramers rate to the symmetric double-humped barrier was recently achieved [7], in which case the activation energy is the arithmetic mean of two partial barriers and the prefactor contains the geometric mean of the starting and the intermediate wells. Such an extension of the Kramers theory has practical importance in the slow relaxation dynamics such as the protein crystallization [1], since the mean barrier height of the activation energy indicates a kind of coherence of the escapes over the partial barriers leading to the enhancement of the nucleation rate due to the existence of the intermediate state [1,2,7]. On the other hand, the transport coefficients such as nonzero particle flow [10], and the diffusion constant [11] in the nonequilibrium steady state of the thermal diffusion in a tilted periodic potential has been studied as a model of ratchet-induced transport [11,12,14]. However, the relaxation dynamics toward the nonequilibrium steady state has not been well examined.

In this paper, as a next step, we explore the Kramers theory for a relaxation dynamics towards the nonequilibrium steady state with the finite current. In particular we analyze the decay rate of a thermal diffusion in a tilted asymmetric periodic potential under the proper periodic boundary condition (PBC), which is a relevant model for the externally loaded motor proteins [13], and obtain a nonequilibrium extension of the Kramers escape rate for double-humped barrier [7].

The decay rate is explored both by the numerical diagonalization of the non-Hermitian Fokker-Planck operator and

by the real and complex WKB analyses with suitable absorbing boundary condition (ABC). There is a range of tilting where the activation energy is given by the arithmetic mean of the partial barrier heights. This fact indicates the coherence of the motion as in the equilibrium relaxation case [7]. Including this case, we treat the whole tilting regime.

This paper is organized as follows. In Sec. II, the relaxation process is formulated as an eigenvalue problem of the Fokker-Planck operator. Especially, asymptotic decay rate is identified with the real part of the first excited eigenvalue. Then, in Sec. III, the decay rates are examined by numerical diagonalization of the Fokker-Planck operator. In Sec. IV, the eigenvalue problem of the Fokker-Planck operator is mapped to that of the associated Schrödinger operator, and at the low temperatures the WKB quantization condition is explored. In particular, the small tilting case is investigated where the potential barriers exist and the eigenvalues are almost real-valued. We show a subtle nonequilibrium extension of the Kramers theory to the tilted double-humped barrier. In Sec. V, we investigate the single barrier case and show that the decay rate obeys a usual Kramers rate despite the presence of nonzero current. In Sec. VI, the large tilting case is analyzed by the WKB quantization for complex eigenvalues. The last section is devoted to discussions.

## II. DECAY RATE IN A TILTED RATCHET

We consider a thermal diffusion process in a tilted ratchet described by the one-dimensional Fokker-Planck equation

$$\frac{\partial}{\partial t}P(x,t) = \frac{1}{\eta} \frac{\partial}{\partial x} \left( \frac{\partial U(x)}{\partial x} + \theta \frac{\partial}{\partial x} \right) P(x,t), \quad (1)$$

where  $P(x,t)$  stands for the probability density with which the Brownian particle is found in a position  $x$  at a time  $t$ . We consider a tilted periodic potential  $U(x) = U^{(0)}(x) - (2\pi W/L)x$  composed of the  $L$ -periodic part  $U^{(0)}(x)$  and the tilting  $W$ .  $W$  takes both positive and negative values.  $\theta$  is the temperature and  $\eta$  is the damping coefficient. For brevity,  $\eta$  is fixed to unity.

As a typical asymmetric potential, we take

\*Electronic address: monnai@suou.waseda.jp

†Electronic address: sugita@a-phys.eng.osaka-cu.ac.jp

‡Electronic address: nakamura@a-phy.eng.osaka-cu.ac.jp

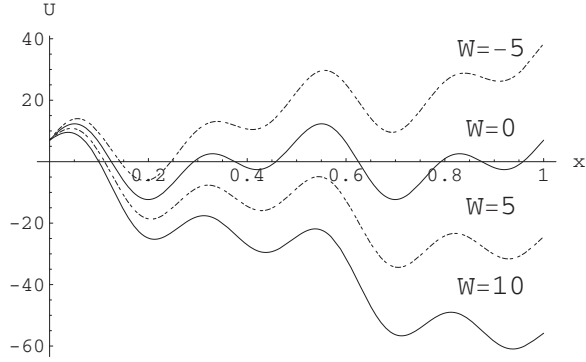


FIG. 1. Tilted periodic potential  $U(x)$  with  $\alpha=1$ ,  $L=1$ , and  $U_0=7$ . The cases of tilting  $W=-5, 0, 5, 10$  are illustrated. For the cases of large negative and large positive biases; see Fig. 5(a) and Fig. 6.

$$U(x) = U_0 \left( \cos \frac{4\pi}{L}x + \alpha \sin \frac{8\pi}{L}x \right) - \frac{2\pi W}{L}x. \quad (2)$$

In order to see the asymptotic decay to the steady state, we take  $L$ -periodic boundary. Since the period of  $\cos(4\pi/L)x + \alpha \sin(8\pi/L)x$  is exactly half of  $L$ ,  $U(x)$  possesses several potential barriers within one period  $L$  of boundary condition. The sinusoidal potential  $U_0 \cos(4\pi/L)x$  has a single barrier in the unit cell  $[0, L]$  and the higher Fourier component  $\alpha U_0 \sin(8\pi/L)x$  yields extra barriers. The shape of the potential is sensitive to the tilting  $W$ . Indeed, for  $\alpha=1$ , and  $U_0=7$ , there is a double-humped barrier for a period in case of the tilting range  $-14 \leq W \leq 28$  (see Fig. 1). While for  $-42 \leq W \leq -14$ , there is a single-humped barrier [Fig. 5(a)]. For  $28 \leq W$ , no barrier exists (Fig. 6).

By setting  $P(x, t) = P(x)e^{-\lambda t}$ , the Fokker-Planck equation becomes the eigenvalue problem:

$$\frac{\partial}{\partial x} \left( \frac{\partial U(x)}{\partial x} + \theta \frac{\partial}{\partial x} \right) P(x) = -\lambda P(x). \quad (3)$$

Since the steady state does not depend on time, the lowest eigenvalue is zero and the real part of the second lowest eigenvalue  $\Gamma \equiv \text{Re}\{\lambda_1\}$  is the asymptotic decay rate to the nonequilibrium steady state. Note that due to the tilting, the eigenvalues are now complex-valued, though its imaginary part is negligibly small compared to the real part for small-enough tilting. If the tilting is large and the barriers disappear, then the imaginary part of the eigenvalue becomes non-negligible. Increasing the tilting near the threshold for the existence of the barriers, the imaginary part of the eigenvalue drastically changes.

### III. NUMERICAL ANALYSIS OF THE DECAY RATE

Let us expand arbitrary tilted  $L$ -periodic potential  $\hat{U}(x)$  into the Fourier series:

$$\hat{U}(x) = \sum_n \left( a_n \cos \frac{2\pi n}{L}x + b_n \sin \frac{2\pi n}{L}x \right) - \frac{2\pi W}{L}x. \quad (4)$$

Then the eigenvalue problem for the Fokker-Planck operator is reduced to the matrix form:

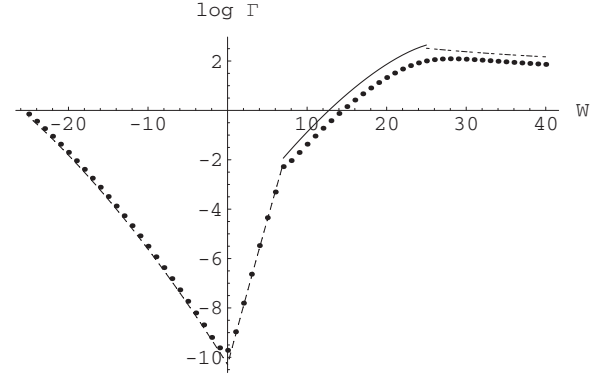


FIG. 2. The series of dots shows the tilting dependence of the numerical decay rate  $\Gamma$  under the fixed parameters  $\alpha=1$ ,  $L=1$ ,  $U_0=7$ , and  $\theta=0.7$ . The tilting range  $-14 \leq W \leq 28$  corresponds to the double-humped barrier case: In the case (i) where the tunnel term is dominant, the analytic formula for the decay rate (24) obtained by WKB analysis is indicated as a solid line. In the case (ii) where the tunneling term is much smaller than the difference of the vacuum energies  $|E_a - E_c|$ , the activation energy calculated as the actual barrier height divided by  $\theta$  is shown as the broken line. For the large negative tiltings, the decay rate obeys Eq. (31) for the single-humped barrier. For large tilting  $28 \leq W$ , the decay rate agrees with the perturbative solution (39) of the complex-valued WKB quantization condition (33) (line in the rightmost region).

$$\sum_m A_{nm} c_m = \lambda c_n,$$

$$A_{nm} = - \left( \frac{2\pi}{L} \right)^2 \left\{ (\theta n^2 + Wni) \delta_{n,m} + \sum_k \left( \frac{nk}{2} a_k - \frac{ink}{2} b_k \right) \delta_{n,m+k} - \sum_k \left( \frac{nk}{2} a_k + \frac{ink}{2} b_k \right) \delta_{-n,k-m} \right\}. \quad (5)$$

The eigenvalue  $\lambda$  of the Fokker-Planck operator is obtained by numerically diagonalizing the matrix  $A_{nm}$  in Eq. (5). In particular, the decay rate  $\Gamma$  is obtained in Fig. 2 for a tilted periodic potential with  $a_2 = U_0$ , and  $b_4 = \alpha U_0$ ,  $U(x) = U_0 [\cos(4\pi/L)x + \alpha \sin(8\pi/L)x] - (2\pi W/L)x$  for tilting range  $-25 \leq W \leq 40$  under the fixed parameters  $U_0=7$ ,  $L=1$ ,  $\alpha=1$ , and  $\theta=0.7$ .

### IV. WKB ANALYSIS OF THE DECAY RATE: SMALL TILTING CASE

The eigenvalue problem of the Fokker-Planck operator is transformed into that of the Schrödinger operator via the so-called separation ansatz,  $P(x) = e^{-U(x)/2\theta} \phi(x)$

$$\theta \phi''(x) + [\lambda - V(x)] \phi(x) = 0, \quad (6)$$

where  $\theta$  plays the role of the Planck-constant  $\hbar \equiv \sqrt{2m\theta}$  with the effective mass  $m$ , and the effective potential  $V(x) \equiv \theta \{ [U'(x)/2\theta]^2 - U''(x)/2\theta \}$  is spatially periodic.

Note that the wave function  $\phi(x)$  should satisfy the boundary condition consistent with the PBC for  $P(x)$  in Eq. (2), and  $\phi(x)$  should exponentially decay (or grow) as  $\phi(x)$

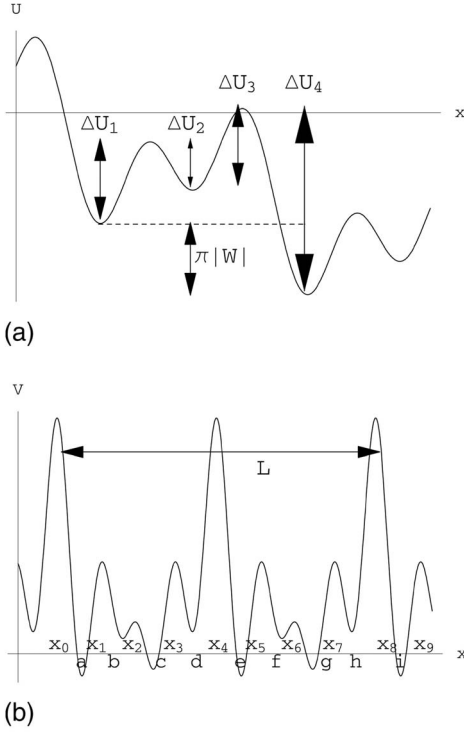


FIG. 3. (a) Schematic illustration of the tilted periodic double-humped barrier with a dip. There are four partial barrier heights  $\Delta U_1, \Delta U_2, \Delta U_3$ , and  $\Delta U_4$ . The actual barrier height is  $\Delta U_4 - \pi|W|$ . (b) Effective periodic potential of the Schrödinger operator corresponding to Fig. 3(a).

$+L) = e^{-\pi W/\theta} \phi(x)$ , since in the separation ansatz, the tilting term yields the exponential factor as  $e^{-U(x+L)/2\theta} = e^{\pi W/\theta} e^{-U(x)/2\theta}$ . Consequently, we explore the eigenvalue problem for the associated Schrödinger operator by assuming the exponentially decaying (or growing) eigenfunction,

$$\phi(x+L) = e^{-\pi W/\theta} \phi(x). \quad (7)$$

If the tilting is small so that the barriers and the local minima of the original potential  $U(x)$  exist, the imaginary part of the eigenvalue  $\lambda$  is negligible compared to the real part. Thus, in this case, we may regard the eigenvalue  $\lambda$  as real and thus identify it with the decay rate  $\Gamma$ . In particular, our interest lies in the high-enough barrier case, i.e., the low temperature case.

### A. Double-humped barrier case

The original potential  $U(x)$  has a double-humped barrier in the absence of tilting  $W=0$ . Thus we first explore the small tilting region with the double-humped barrier, as schematically shown in Fig. 3(a). Since the temperature is low, we use the WKB approximation for the associated Schrödinger operator. The first excited state connects localized states in all the wells  $a, c, e, g$ , and  $i$  of  $V(x)$  in Fig. 3(b).

Let us denote the wavefunctions in the regions,  $a, b, c, d, e, f, g, h$  and  $i$  bordered by the classical turning points,  $x_0, \dots, x_9$  as  $\phi_a(x), \dots, \phi_i(x)$ , respectively [see Fig. 3(b)]. In general, near the classical turning point  $x=z_0$ , the

wave function is connected by the connection formula

$$\begin{aligned} & \frac{1}{\sqrt{p}} e^{\pm i[(1/\hbar)\int_{z_0}^x p dy + (\pi/4)]} [E > V(x)] \\ & \leftrightarrow \frac{1}{\sqrt{p}} \left( e^{(1/\hbar)\int_{z_0}^x p dy} \pm \frac{i}{2} e^{-(1/\hbar)\int_{z_0}^x p dy} \right) [E < V(x)], \\ & p(x) = \sqrt{2m|\lambda - V(x)|}. \end{aligned} \quad (8)$$

The wave function in the leftmost region  $\phi_a(x) = (1/\sqrt{p}) \times (c_1 e^{-(i/\hbar)\int_{x_0}^x p(y) dy} + c_2 e^{(i/\hbar)\int_{x_0}^x p(y) dy})$  is connected successively to that of the middle region  $e$  as  $\phi_e(x) = (1/\sqrt{p}) [(Ac_1 + Bc_2) e^{-(i/\hbar)\int_{x_d}^x p(y) dy} + (Cc_1 + Dc_2) e^{(i/\hbar)\int_{x_d}^x p(y) dy}]$ , where the coefficients  $A, B, C$ , and  $D$  are expressed as

$$\begin{aligned} A &= e^{iS_a} \left\{ \frac{1}{2} \left( i e^{M_b} \sin S_c + \frac{1}{4} e^{-M_b} \cos S_c \right) e^{-M_d} \right. \\ & \quad \left. + 2 \left( e^{M_b} \cos S_c + \frac{i}{4} e^{-M_b} \sin S_c \right) e^{M_d} \right\}, \\ B &= e^{-iS_a} \left\{ \frac{1}{2} \left( e^{M_b} \sin S_c + \frac{i}{4} e^{-M_b} \cos S_c \right) e^{-M_d} \right. \\ & \quad \left. - 2 \left( i e^{M_b} \cos S_c + \frac{1}{4} e^{-M_b} \sin S_c \right) e^{M_d} \right\}, \\ C &= e^{iS_a} \left\{ \frac{1}{2} \left( e^{M_b} \sin S_c - \frac{i}{4} e^{-M_b} \cos S_c \right) e^{-M_d} \right. \\ & \quad \left. - 2 \left( -i e^{M_b} \cos S_c + \frac{1}{4} e^{-M_b} \sin S_c \right) e^{M_d} \right\}, \\ D &= e^{-iS_a} \left\{ \frac{1}{2} \left( -i e^{M_b} \sin S_c + \frac{1}{4} e^{-M_b} \cos S_c \right) e^{-M_d} \right. \\ & \quad \left. + 2 \left( e^{M_b} \cos S_c - \frac{i}{4} e^{-M_b} \sin S_c \right) e^{M_d} \right\}. \end{aligned} \quad (9)$$

Here the actions for the well-regions  $\alpha = a, c, e, g$ , and  $i$  are given as  $S_\alpha \equiv \int_{x_{\alpha-}}^{x_{\alpha+}} \sqrt{\theta^{-1}[\lambda - V(x)]} dx$ , and the tunnel integrals are  $M_\beta \equiv M_b = M_d = \int_{x_{\beta-}}^{x_{\beta+}} \sqrt{\theta^{-1}[V(x) - \lambda]} dx$ . Here we used the abbreviated notations, for the well region  $\alpha = a, c, e$ , and for the barrier region  $\beta = b, d$ , which is bordered by the classical turning points  $x_{\alpha-/\beta-}$  and  $x_{\alpha+/\beta+}$ . Then, in the same way, the localized wave function  $\phi_e(x)$  is successively connected to that of the rightmost region  $i$  as  $\phi_i(x) = (1/\sqrt{p}) [(A'c_1 + B'c_2) e^{-(i/\hbar)\int_{x_g}^x p(y) dy} + (C'c_1 + D'c_2) e^{(i/\hbar)\int_{x_g}^x p(y) dy}]$ . Here, due to the periodicity of  $V(x)$ , the set of the coefficients  $\{A', B', C', D'\}$  is given by

$$\begin{pmatrix} A' & B' \\ C' & D' \end{pmatrix} = \begin{pmatrix} A & B \\ C & D \end{pmatrix}^2. \quad (10)$$

The periodicity of the potential  $V(x)$  demands the Floquet-type condition,  $\phi_i(x+L) = e^{iKL} \phi_a(x)$ . Due to the ex-

ponentially decaying condition (7),  $K$  has the imaginary part

$$K = i \frac{\pi W}{\theta L}. \quad (11)$$

Here the real part of  $K$  is zero under the PBC. This relation gives a constraint to guarantee the nontrivial coefficients  $(c_1, c_2)$  of  $\phi_a$  and  $\phi_i$ :

$$\begin{vmatrix} A' - e^{iKL} & B' \\ C' & D' - e^{iKL} \end{vmatrix} = 0, \quad (12)$$

which can be rewritten as

$$e^{\pi W/\theta} = \frac{1}{2}(A' + D') \pm \sqrt{\frac{1}{4}(A' + D')^2 - 1} \approx A' + D' \quad (13)$$

or

$$(A' + D')^{-1},$$

with use of the relation  $A'D' - B'C' = 1$ . Now let us consider the eigenvalues  $(\Lambda_1, \Lambda_2)$  of the coefficient matrix,

$$\begin{pmatrix} A' & B' \\ C' & D' \end{pmatrix}. \quad (14)$$

From the relation  $A'D' - B'C' = 1$ , one has  $\Lambda_2 = \Lambda_1^{-1}$ . Since the trace is given as  $A' + D' = \Lambda_1 + \Lambda_1^{-1}$ , the boundary condition (13) requires

$$e^{\pi W/\theta} \approx \Lambda_1 + \Lambda_1^{-1} \quad \text{or} \quad (\Lambda_1 + \Lambda_1^{-1})^{-1}, \quad (15)$$

and numerical results tells us that we should take one of the branches according to the sign of the tilting  $W$  as

$$e^{\pi W/\theta} \approx \Lambda_1 + \Lambda_1^{-1} \quad (W > 0),$$

$$e^{\pi W/\theta} \approx (\Lambda_1 + \Lambda_1^{-1})^{-1} \quad (W < 0). \quad (16)$$

Thus one has  $(\Lambda_1, \Lambda_2) \approx (e^{\pm \pi W/\theta}, e^{\mp \pi W/\theta})$  and the boundary condition (13) turns out to be

$$e^{\pi |W|/\theta} \approx A' + D'. \quad (17)$$

Substituting the leading term of Eq. (9) into Eq. (17), we obtain the equation

$$e^{2M_b} e^{2M_d} \cos^2(S_a) \cos^2(S_c) = e^{\pi |W|/\theta}. \quad (18)$$

Due to the small transparency of the barrier, the action is almost quantized as  $S_\alpha \approx \pi(n_\alpha + \frac{1}{2})$ , and hence

$$\begin{aligned} \cos S_\alpha &= (-1)^{n_\alpha+1} [S_\alpha - \pi(n_\alpha + 1/2)] \\ &+ O([S_\alpha - \pi(n_\alpha + 1/2)]^3). \end{aligned} \quad (19)$$

The harmonic approximation around the minima of  $V(x)$  in the region  $a$ ,  $x = x_{\min}^a$ , and that of region  $c$ ,  $x = x_{\min}^c$  give

$$S_\alpha(\lambda) \approx (\lambda - E_\alpha) \left. \frac{dS}{dE} \right|_{E_\alpha} + S(E_\alpha) = \pi \frac{\lambda - V(x_{\min}^\alpha)}{\hbar \omega_\alpha}, \quad (20)$$

with the vacuum energy  $E_\alpha \equiv \hbar \omega_\alpha/2 + V(x_{\min}^\alpha)$ , the action at vacuum energy  $S(E_\alpha) = \pi/2$  with  $n_\alpha = 0$ , and the frequency

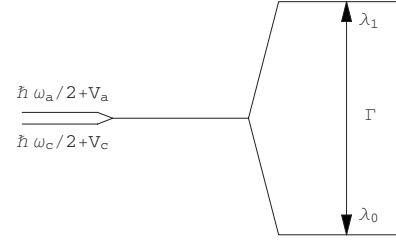


FIG. 4. Tunnel splitting of the degenerated lowest two eigenvalues,  $\lambda_1$  and  $\lambda_0$ . Since we consider single barrier case, the lowest two eigenvalues are degenerate.

$\omega_\alpha \equiv \sqrt{m^{-1}V''(x_{\min}^\alpha)}$ . Substituting Eq. (19) and Eq. (20) into Eq. (18), one has

$$\begin{aligned} e^{2M_b} e^{2M_d} \{ \pi[\lambda - V(x_{\min}^a)]/\hbar \omega_a - \pi(n_a + 1/2) \}^2 \\ \times \{ \pi[\lambda - V(x_{\min}^c)]/\hbar \omega_c - \pi(n_c + 1/2) \}^2 = e^{\pi |W|/\theta}. \end{aligned} \quad (21)$$

The lowest two eigenvalues  $0 = \lambda_0 < \lambda_1$  are thus the solutions of the polynomial equation (21) with  $n_a = n_c = 0$ ,

$$\lambda = \frac{1}{2} \left( E_a + E_c \pm \sqrt{(E_a - E_c)^2 + \frac{4\hbar^2 \omega_a \omega_c}{\pi^2} e^{\pi |W|/2\theta - M_b - M_d}} \right). \quad (22)$$

There are two typical cases of level splitting

(i) The case where the tunneling term is much larger than the difference of the vacuum levels:  $|E_a - E_c| \ll \sqrt{4\hbar^2 \omega_a \omega_c / \pi^2} e^{\pi |W|/4\theta - (M_b + M_d)/2}$ .

(ii) The case where the tunneling term is much smaller than the difference of the vacuum levels:  $|E_a - E_c| \gg \sqrt{4\hbar^2 \omega_a \omega_c / \pi^2} e^{\pi |W|/4\theta - (M_b + M_d)/2}$ .

First, we investigate the former case (i). The degeneracy of the lowest two eigenvalues is removed due to the tunneling term (see Fig. 4). The decay rate  $\Gamma$  is obtained as the difference between the first excited level  $\lambda_1$  and the ground level  $\lambda_0$  as

$$\Gamma = \lambda_1 - \lambda_0 = \frac{2\sqrt{\hbar \omega_a \hbar \omega_c}}{\pi} e^{\pi |W|/4\theta - (M_b + M_d)/2}. \quad (23)$$

The details of the evaluations of the curvature  $\hbar \omega_\alpha$  and tunneling integral  $M_\beta$  are shown in Appendix A. With use of Eq. (23), Eq. (A2), and Eq. (A4), we obtain the decay rate  $\Gamma$ , which is a subtle nonequilibrium extension of the so-called Kramers rate [7,12,8]

$$\begin{aligned} \Gamma &= \frac{2}{\pi} e^{2-\sqrt{2}-\text{arcsinh}(1)} [U''(x_{\min}^a) U''(x_{\min}^c) |U''(x_{\max}^b) U''(x_{\max}^d)|]^{1/4} \\ &\times e^{[\pi |W| - (\Delta U_1 + \Delta U_2 + \Delta U_3 + \Delta U_4)]/4\theta} \end{aligned} \quad (24)$$

with the partial barriers  $\Delta U_1 = U(x_{\max}^b) - U(x_{\min}^a)$ ,  $\Delta U_2 = U(x_{\max}^b) - U(x_{\min}^c)$ ,  $\Delta U_3 = U(x_{\max}^d) - U(x_{\min}^c)$ , and  $\Delta U_4 = U(x_{\max}^d) - U(x_{\min}^a)$  (see Fig. 3). We notice that the original potential has a unique maximum  $x = x_{\max}^\beta$  between the classical turning points neighboring to the region  $\beta$ ,  $x_{\beta_-}$ , and  $x_{\beta_+}$ . Although the actual barrier height is the minimum of  $\Delta U_{1,2,3}$

and  $\Delta U_4 - \pi|W|$ , the activation energy is the arithmetic mean of the four partial barrier heights. On the other hand, the prefactor is the geometric mean of the curvatures at the minima and the maxima. Thus the above Kramers type decay rate (24) is taken as a nonequilibrium extension of [7], which agrees with the numerical decay rate (see Fig. 2).

$$\lambda = E_a \pm \frac{2\hbar^2 \omega_a \omega_c}{\pi^2 |E_a - E_c|} e^{\pi|W|/2\theta - M_b - M_d} \quad \text{or} \quad E_c \pm 2\hbar^2 \omega_a \omega_c / \pi^2 |E_a - E_c| e^{\pi|W|/2\theta - M_b - M_d}, \quad (25)$$

which splits by the tunnel term. The decay rate  $\Gamma$  is

$$\begin{aligned} \Gamma &= \frac{2U''(x_{\min}^a)U''(x_{\min}^c)}{\pi^2 |E_a - E_c|} e^{\pi|W|/2\theta - M_b - M_d} = \frac{\sqrt{U''(x_{\min}^a)U''(x_{\min}^c)}|U''(x_{\max}^b)U''(x_{\max}^d)|}{\pi^2 |E_a - E_c|} e^{4-2\sqrt{2}-2 \operatorname{arcsinh}(1)} e^{\pi|W|/2\theta - (\Delta U_1 + \Delta U_2 + \Delta U_3 + \Delta U_4)/2\theta} \\ &= \frac{\sqrt{U''(x_{\min}^a)U''(x_{\min}^c)}|U''(x_{\max}^b)U''(x_{\max}^d)|}{\pi^2 |E_a - E_c|} e^{4-2\sqrt{2}-2 \operatorname{arcsinh}(1)} e^{-(\Delta \tilde{U}_1 + \Delta \tilde{U}_2)/\theta}, \end{aligned} \quad (26)$$

where taking it into consideration that  $\Delta \tilde{U}_1 = (\Delta U_1 + \Delta U_2)/2$  and  $\Delta \tilde{U}_2 = (\Delta U_3 + \Delta U_4 - \pi|W|)/2$  correspond to the left and the right barriers' heights, respectively. Thus the activation energy can be regarded as the sum of the barrier heights, i.e., the decay rate is given by the product of the escape rates over the left and right barriers. This fact is interpreted as the independence or incoherence of the escapes over the left and the right barriers. The prefactor can not be expressed only by the original potential  $U(x)$ . The activation energy calculated as the actual barrier height divided by the temperature agrees with the numerical result as in Fig. 2.

### B. Single-humped barrier case

For slightly large negative tilting, the dip of the barrier of the potential (2) disappears, and there is a single-humped barrier as shown in Fig. 5(a). The decay rate for the tilted single barrier can be evaluated in the same way as the case of the double-humped barrier. The effective potential  $V(x)$  has a single barrier in a period. The localized wave function in the left-most region  $\phi_a(x) = (1/\sqrt{p})(c_1 e^{-(i\hbar) \int_{x_0}^x p(y) dy} + c_2 e^{(i\hbar) \int_{x_0}^x p(y) dy})$  is connected successively to that of the rightmost region as

$$\begin{aligned} \phi_e(x) &= \frac{1}{\sqrt{p}} \left[ (A c_1 + B c_2) e^{-(i\hbar) \int_{x_4}^x p(y) dy} \right. \\ &\quad \left. + (C c_1 + D c_2) e^{(i\hbar) \int_{x_4}^x p(y) dy} \right], \end{aligned}$$

where the coefficients  $A$ ,  $B$ ,  $C$ , and  $D$  are given by Eq. (9). The Froquet-type relation which express the absorbing boundary condition is

$$e^{\pi|W|/\theta} = A + D = \Lambda'_1 + \Lambda'_2, \quad (27)$$

with the eigenvalues  $\Lambda'_1$ , and  $\Lambda'_2$  of the coefficient matrix

Now we consider the case (ii) and show the corresponding decay rate. The argument is parallel to the case (i) except for the evaluation of the square root of Eq. (22), which in the case (ii) expanded as  $|E_a - E_c| (1 + [2\hbar^2 \omega_a \omega_c / (\pi^2 |E_a - E_c|^2)]) e^{\pi|W|/2\theta - M_b - M_d}$ . The energy level is given as

$$\begin{pmatrix} A & B \\ C & D \end{pmatrix}. \quad (28)$$

Then in the same way as in the previous subsection, one has

$$4e^{2M_\beta} \cos^2 S_a = e^{\pi|W|/\theta}. \quad (29)$$

From the small transparency of the barriers and the harmonic approximation of the action with respect to the eigenvalue, Eq. (29) gives the energy levels

$$\lambda = \sqrt{2\theta V''(x_{\min})} \left( n + \frac{1}{2} \right) + V(x_{\min}) \pm \frac{\sqrt{\theta V''(x_{\min})}}{\pi} e^{\pi|W|/2\theta - M}, \quad (30)$$

where we omitted the subscripts since the set of wells and the barriers of effective potential  $V(x)$  are exactly identical. As in [5], the decay rate  $\Gamma$  is given by the difference of the lowest two levels.

After the straightforward calculation, one has

$$\Gamma = \frac{1}{\pi} e^{2-\sqrt{2}-\operatorname{arcsinh}(1)} \sqrt{U''(x_{\min})|U''(x_{\max})|} e^{-\Delta U/\theta} \quad (31)$$

to the lowest order of  $\theta$ , which agrees with the numerical results (cf. Fig. 2). In spite of the presence of the finite current, the activation energy is exactly the actual barrier height  $\Delta U$  measured from the bottom of the local minimum [see Fig. 5(a)], which is the case encountered in the usual Kramers theory based on the escape rate formalism.

### V. WKB ANALYSIS: LARGE TILTING CASE

In the large tilting case where the original potential  $U(x)$  has no barriers (cf. Fig. 6), the imaginary part of the eigenvalue  $E_2 = \operatorname{Im}\{\lambda\}$  becomes comparable to the real part  $E_1 = \operatorname{Re}\{\lambda\}$ . Hence we should use the WKB analysis with com-

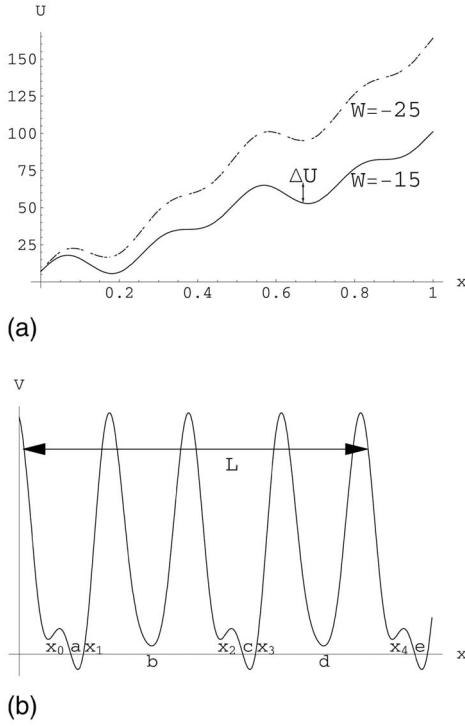


FIG. 5. (a) The single-humped barrier with fixed parameters,  $U_0=7$ ,  $\theta=0.7$ ,  $L=1$ , and  $\alpha=1$ . Both for  $W=-15$  and  $W=-25$ , there is a single-humped barrier  $\Delta U$  measured from the local minimum. (b) The schematic illustration of the effective potential for the single-humped barrier case. In contrast to the double-humped barrier case, there are only two well-regions within a period.

plex energy. Expanding the action to the second order in the effective Planck-constant  $\hbar$ , the eigenfunction of the associated Schrödinger operator is

$$\phi(x) = e^{(i\hbar)[S_0 + (\hbar/i)S_1]} = \frac{C}{\sqrt{p(x)}} e^{(i\hbar)\int_0^x p(y)dy}, \quad (32)$$

with  $S_0 = \int_0^x p(y)dy$ ,  $S_1 \propto -\frac{1}{2} \log p(x)$  and  $p(x) = \sqrt{E_1 - V(x) + iE_2}$ . Therefore such a quantization condition is given as [15]

$$e^{\pm i\int_0^L \sqrt{\theta^{-1}[E_1 + iE_2 - V(x)]} dx} = e^{-\pi W/\theta \pm 2\pi i}. \quad (33)$$

Since the numerical eigenvalue has, in the wide parameter range, the phase factor  $n=1$ , and thus we assume  $n$  is unity. The quantization condition (33) is rewritten into a nonalgebraic equation

$$\int_0^L \sqrt{\theta^{-1}[V(x) - E_1 - iE_2]} dx = -\frac{\pi W}{\theta} + 2\pi i. \quad (34)$$

Because of the low temperature, we neglect the term  $U''(x)/2$  in the effective potential  $V(x) = U'(x)^2/4\theta - U''(x)/2$ . Then we perturbatively solve Eq. (34) (see also [15]) with the expansion parameter  $\epsilon = U_0/W$ . Equation (34) is transformed into the set of equations

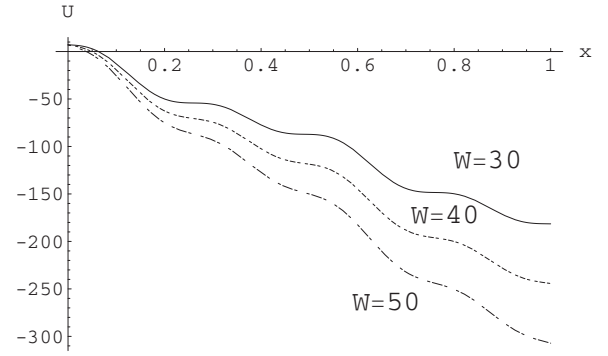


FIG. 6. The tilted potentials without barriers are illustrated for  $W=30, 40$ , and  $50$ , with fixed parameters  $U_0=7$ ,  $\theta=0.7$ ,  $L=1$ , and  $\alpha=1$ .

$$\int_0^L \sqrt{\frac{1}{2}(I_1 + \sqrt{I_1^2 + I_2^2})} dx = L, \quad (35)$$

$$\int_0^L \sqrt{\frac{1}{2}(-I_1 + \sqrt{I_1^2 + I_2^2})} dx = \pm \frac{2\theta L}{W} i,$$

with

$$I_1 = \left[ 1 + \epsilon \left( 2 \sin \frac{4\pi}{L} x - 4\alpha \cos \frac{8\pi}{L} x \right) \right]^2 - \frac{\theta L^2}{W^2 \pi^2} E_1, \quad (36)$$

$$I_2 = \frac{\theta L^2}{W^2 \pi^2} E_2.$$

Expanding the eigenvalues  $E_1 + iE_2$  into the series of  $\epsilon$  as

$$\frac{\theta L^2}{W^2 \pi^2} E_1 = A_1 \epsilon + A_2 \epsilon^2 + A_3 \epsilon^3 + A_4 \epsilon^4 + O(\epsilon^5), \quad (37)$$

$$\frac{\theta L^2}{W^2 \pi^2} E_2 = B_1 \epsilon + B_2 \epsilon^2 + B_3 \epsilon^3 + B_4 \epsilon^4 + O(\epsilon^5),$$

straightforward calculation shows that

$$A_1 = 0, \quad A_2 = \frac{4\theta^2}{U_0^2}, \quad A_3 = 0, \quad A_4 = \frac{24\theta^2}{U_0^2} (1 + 4\alpha^2),$$

$$B_1 = \pm \frac{4\theta}{U_0}, \quad B_2 = 0, \quad B_3 = \mp \frac{8\theta}{U_0} (1 + 4\alpha^2). \quad (38)$$

Thus to the second order of perturbation, the eigenvalue is given as

$$E_1 = \left( \frac{2\pi}{L} \right)^2 \frac{\theta}{\eta} + 24(1 + 4\alpha^2) \left( \frac{\pi U_0}{WL} \right)^2 \frac{\theta}{\eta}, \quad (39)$$

$$E_2 = \pm \left[ \left( \frac{2\pi}{L} \right)^2 \frac{W}{\eta} - \frac{8(1 + 4\alpha^2)\pi^2}{L^2 W \eta} U_0^2 \right]. \quad (40)$$

In particular, the real part accurately gives the numerical decay rate (see large positive tilting range in Fig. 2). As expected, the leading terms give the first excited eigenvalue  $(2\pi/L)^2(\theta + iW)/\eta$  for the case of  $U_0=0$ .

We should notice that the quantization condition (33) is valid essentially in the absence of the barriers, since it is not concerned with the classical turning points.

## VI. DISCUSSION

The low-temperature relaxation dynamics has been revisited in the context of the Kramers theory. Stimulated by the subtle extension of the Kramers rate in the system with the well-defined thermal equilibrium but accompanied with the intermediate state [1,2,7], we here explored the case of the asymmetric periodic potential under a constant external bias.

Since our interest lies in the slow dynamics, the low temperature and thus the high-enough barrier are assumed. Then we have explored the nonequilibrium extension of the Kramers theory with the aid of WKB analysis. There are four regime of the decay rate and we have obtained the formulas (24), (26), (31), and (39) for the respective cases. Equations (24) and (26) correspond to the case with a double-humped barrier. Equations (31) and (39) correspond to the single-humped barrier and no barrier cases, respectively. The relaxation process in the tilted double-humped barrier is composed of two cases. In the case (i) where tunnel-term is dominant, the WKB analysis under the absorbing boundary condition gives the analytic expression (24) for the decay rate. The activation energy is given by the arithmetic mean height of four partial barriers, which is certainly lower than the actual barrier height. This is considered as the enhancement of the relaxation due to a kind of coherence of the escapes over individual barriers. In the case (ii) where the tunneling term is much smaller than the typical difference of vacuum energy levels, the activation energy is given by Eq. (26). The single-humped barrier case is analyzed as well and, in spite of the presence of the finite current, the decay rate is the usual Kramers escape rate encountered in the relaxation to equilibrium state.

On the other hand, if we increase the bias  $W$  beyond the threshold for the existence of the barriers, the decay rate  $\Gamma$  does immediately deviate from the Arrhenius plot. Such a large tilting case is accurately treated with use of the WKB quantization condition with complex eigenvalues (33).

The decay rate strongly depends on the direction of the tilting, i.e., decay rates are largely different between the tiltings  $\pm W$ . In other words, there are situations where negatively biased system with the tilting  $-W$  is in the small tilting region possessing the barrier and obeys Eq. (31), while the positively biased system with the tilting  $W$  has no barrier and thus is in the large tilting case which is treated by the WKB analysis with complex energy Eq. (39). On the other hand, the steady state particle current [10]

$$\langle \dot{x} \rangle = N(1 - e^{-2\pi W/\theta})$$

$$N \equiv L \frac{\theta}{\eta} \left( \int_0^L dx \int_x^{x+L} dy e^{\frac{U(y)-U(x)}{\theta}} \right)^{-1} \quad (41)$$

shows quite similar asymmetric tilting dependence as the decay rate, since it is given as the difference between Kramers escape rates for the positive and negative directions of the

bias [12]. The decay rate  $\Gamma$  gives the time scale for a Brownian particle to escape from the present local minimum to the neighboring one. Thus the asymmetry of the decay rate as well as that of the steady-state current with respect to the direction of bias is favorable for rectification of the particle flow in the presence of time-dependent stochastic or deterministic perturbations. The quantitative study of the relation between the relaxation dynamics and the transports including time-dependent ratchets would be made in due course.

## ACKNOWLEDGMENTS

T.M. owes much to JSPS and the 21st Century COE Program (Holistic Research and Education Center for Physics of Self-Organization Systems) both from the Ministry of Education, Culture, Sports, Science, and Technology of Japan. A.S. and K.N. are grateful to JSPS for the financial support for fundamental research.

## APPENDIX A: EVALUATION OF THE CURVATURES AND TUNNELING INTEGRALS

The curvature  $\hbar\omega_\alpha$  is evaluated as follows. Omitting the tunneling term, one has

$$0 \approx \frac{\hbar\omega_\alpha}{2} + V(x_{\min}^\alpha) = \frac{\sqrt{2\theta V''(x_{\min}^\alpha)}}{2} + V(x_{\min}^\alpha), \quad (A1)$$

thus, with use of  $U'(x_{\min}^\alpha) = 0$ ,

$$\hbar\omega_\alpha = \sqrt{2\theta V''(x_{\min}^\alpha)} \approx -U_0 \left( \frac{2\pi}{L} \right)^2 \left( 4 \cos \frac{4\pi}{L} x_{\min}^\alpha + 16 \sin \frac{8\pi}{L} x_{\min}^\alpha \right) = U''(x_{\min}^\alpha). \quad (A2)$$

Since the temperature is low, the tunneling integral  $M_\beta$  is evaluated in the first order of the temperature  $\theta$  as

$$\begin{aligned} \theta M_\beta &= \int_{x_{\beta-}}^{x_{\beta+}} \sqrt{\left( \frac{U'(x)}{2} \right)^2 - \theta \frac{U''(x)}{2} - \lambda \theta} dx \\ &\approx \left\{ \int_{x_{\beta-}}^{x_{\max}^\beta - \Delta} + \int_{x_{\max}^\beta - \Delta}^{x_{\max}^\beta + \Delta} + \int_{x_{\max}^\beta + \Delta}^{x_{\beta+}} \right\} \\ &\quad \times \sqrt{\left( \frac{U'(x)}{2} \right)^2 - \theta \frac{U''(x)}{2}} dx \\ &= \int_{x_{\beta-}}^{x_{\max}^\beta - \Delta} \left( \frac{U'(x)}{2} - \frac{\theta U''(x)}{2U'(x)} \right) dx \\ &\quad + \int_{-\Delta}^{\Delta} \sqrt{\frac{\theta |U''(x_{\max}^\beta)|}{2}} \sqrt{1 + \frac{|U''(x_{\max}^\beta)|}{2\theta}} y^2 dy \\ &\quad + \int_{x_{\max}^\beta + \Delta}^{x_{\beta+}} \left( -\frac{U'(x)}{2} + \frac{\theta U''(x)}{2U'(x)} \right) dx + O(\theta^2) \\ &= \frac{1}{2} [2U(x_{\max}^\beta) - U(x_{\beta-}) - U(x_{\beta+})] + \theta \left\{ \sqrt{2} + \operatorname{arcsinh}(1) \right\} \end{aligned}$$

$$-1 - \frac{1}{2} \log[2\theta|U''(x_{\max}^{\beta})|/|U'(x_{\beta-})|U'(x_{\beta+})|] + O(\theta^2). \quad (\text{A3})$$

In the square root of the integrand on the second term,  $\theta\lambda$  is small compared to the first two terms and is omitted. The integral is divided into the one around the maximum,  $[x_{\max}^{\beta}$

$-\Delta, x_{\max}^{\beta} + \Delta]$  with the width  $\Delta \equiv \sqrt{2\theta/|U''(x_{\max}^{\beta})|}$  and remaining ones. It should be noticed that in the lowest order of  $\theta$ , the arithmetic mean of the left and right barrier heights can be found in the final result in Eq. (A3).

The classical turning points  $x_1, x_2$  is evaluated as  $x_1 = x_{\min}^a - \sqrt{2\theta/U''(x_{\min}^a)}$  and  $x_2 = x_{\max}^b - \sqrt{2\theta/U''(x_{\max}^b)}$ . Thus the tunnel integral  $M_{\beta}$  is given by

$$\theta M_{\beta} \approx \frac{1}{2}[2U(x_{\max}^{\beta}) - U(x_{\min}^{\beta-}) - U(x_{\min}^{\beta+})] + \theta \left\{ \sqrt{2} + \operatorname{arcsinh}(1) - 2 - \frac{1}{2} \log[|U''(x_{\max}^{\beta})|/\sqrt{U''(x_{\min}^{\beta-})U''(x_{\min}^{\beta+})}] \right\}. \quad (\text{A4})$$

The minimum and the maximum points  $x_{\min}^{\beta\pm} \equiv x_{\min}^{a/c}$ , and  $x_{\max}^b$  are calculated as  $x_{\min}^a = L/4 - G_+(W)$  and  $x_{\max}^b = L/4 - G_-(W)$ , with  $G_{\pm}(W) = (L/4\pi) \arcsin[(-1 \pm \sqrt{1 - 8\alpha W/U_0 + 32\alpha^2})/8\alpha]$ .

In the same way, for the well region  $c$ , the classical turning points and the minimum and the maximum points are calculated.

- 
- [1] O. Galkin and P. G. Vekilov, *J. Cryst. Growth* **232**, 63 (2001).  
 [2] G. Nocolis and C. Nocolis, *Physica A* **323**, 139 (2003).  
 [3] R. Kapral, in *New Trends in Kramers' Reaction Rate Theory*, edited by P. Talkner and P. Hänggi (Kluwer Academic Publishers, Dordrecht, 1995), pp. 107.  
 [4] R. Zwanzig, *Nonequilibrium Statistical Mechanics* (Oxford University Press, Oxford, 2001).  
 [5] N. G. van Kampen, *J. Stat. Phys.* **17**, 71 (1977); *Prog. Theor. Phys. Suppl.* **64**, 389 (1978); *Stochastic Processes in Physics and Chemistry*, 2nd ed. (North-Holland, Amsterdam, 1981).  
 [6] B. Caroli, C. Caroli, and B. Roulet, *J. Stat. Phys.* **21**, 415 (1979); **26**, 83 (1981); H. Tomita, A. Ito, and H. Kidachi, *Prog. Theor. Phys.* **56**, 786 (1976); K. Nakamura and T. Sasada, *Phys. Lett.* **74A**, 379 (1979).  
 [7] T. Monnai, A. Sugita, and K. Nakamura, *Phys. Rev. E* **74**, 061116 (2006).  
 [8] P. Hänggi, P. Talkner, and M. Borkovec, *Rev. Mod. Phys.* **62**, 251 (1990).  
 [9] D ter Haar, *Selected Problems in Quantum Mechanics* (Academic, New York, 1964); S. Ohta and K. Nakamura, *J. Phys. C* **14**, L427 (1981).  
 [10] R. L. Stratonovich, *Radiotekh. Elektron. (Moscow)* **3**, 497 (1958).  
 [11] P. Reimann, C. Van den Broeck, H. Linke, P. Hänggi, J. M. Rubi, and A. Pérez-Madrid, *Phys. Rev. Lett.* **87**, 010602 (2001); *Phys. Rev. E* **65**, 031104 (2002).  
 [12] P. Reimann, *Phys. Rep.* **361**, 57 (2002).  
 [13] E. Heinsalu, T. Örd, and Risto Tammelo, *Phys. Rev. E* **70**, 041104 (2004).  
 [14] G. Lattanzi and A. Maritan, *J. Chem. Phys.* **117**, 10339 (2002).  
 [15] T. Monnai, A. Sugita, J. Hirashima, and K. Nakamura, *Physica D* **219**, 177 (2006).